

Experimental research on the propagation of plastic hinge length for multi-scale reinforced concrete columns under cyclic loading

Zhenyun Tang^{1a}, Hua Ma^{1b}, Jun Guo^{1c}, Yongping Xie^{1,2d} and Zhenbao Li^{1*}

¹The Key Laboratory of Urban Security and Disaster Engineering, Ministry of Education, Beijing University of Technology, Beijing, 100124, China

²College of Exploration Technology and Engineering, Shijiazhuang University of Economics, Shijiazhuang, 050031, China

(Received May 1, 2015, Revised February 5, 2016, Accepted February 24, 2016)

Abstract. The plastic hinge lengths of beams and columns are a critical demand parameter in the nonlinear analysis of structures using the finite element method. The numerical model of a plastic hinge plays an important role in evaluating the response and damage of a structure to earthquakes or other loads causing the formation of plastic hinges. Previous research demonstrates that the plastic hinge length of reinforced concrete (RC) columns is closely related to section size, reinforcement ratio, reinforcement strength, concrete strength, axial compression ratio, and so on. However, because of the limitations of testing facilities, there is a lack of experimental data on columns with large section sizes and high axial compression ratios. In this work, we conducted a series of quasi-static tests for columns with large section sizes (up to 700 mm) and high axial compression ratios (up to 0.6) to explore the propagation of plastic hinge length during the whole loading process. The experimental results show that besides these parameters mentioned in previous work, the plastic hinge of RC columns is also affected by loading amplitude and size effect. Therefore, an approach toward considering the effect of these two parameters is discussed in this work.

Keywords: reinforced concrete column; axial compression ratio; plastic hinge length; loading amplitude; size effect

1. Introduction

The plastic hinge is a typical sign of structural components entering the plastic phase and a fundamental assumption for the elastic–plastic analysis of a structure under seismic action (Inel and Ozmen 2006). It dominates both the internal force redistribution and deformation mechanism when a structure is in the plastic phase. Except in the constitutive model (Inel and Ozmen 2006), the plastic

*Corresponding author, Professor, E-mail: lizb@bjut.edu.cn

^aPh.D., E-mail: tzy@bjut.edu.cn

^bProfessor, E-mail: mahua@bjut.edu.cn

^cM.S. student, E-mail: guojun911205@126.com

^dPh.D., E-mail: axyapa@163.com

hinge length is another demand parameter necessary for accurately obtaining the nonlinear structural response (Mortezaei *et al.* 2013, Scott *et al.* 2006). So far, many scholars have worked on the theoretical description of the plastic hinge length of reinforced concrete (RC) structural components.

In terms of experimental research, Baker (1956) tested more than 90 RC columns considering the axial compression ratio, concrete strength, shear span ratio, and section size. In addition, they created a formula to calculate the plastic hinge length from the measured moment-curvature curves. After that, Ban and Yamada (1958) proposed another calculation method taking into account the effect of section height, reinforcement ratio, reinforcement strength, and concrete strength. Chen *et al.* (1984) thought the tension and compression reinforcement ratios should be considered individually in the calculation of the plastic hinge length of RC columns. Meanwhile, Shen and Weng (1980) gave an approximate range (0.2-0.5 times the section height). Based on the results of Yang *et al.* (2013), this value was around 1.0 times the section height. Zahn's (1985) research results on RC columns with different section shapes showed that the axial compression ratio was an important parameter in the calculation of the plastic hinge length of RC columns. However, Priestley and Park (1987) thought that the bending and bond-slip effects in RC were the principal factors for determining the plastic hinge length of RC columns. Based on this assumption, the plastic hinge length depends on the shear span ratio and reinforcement diameter. Nevertheless, in Paulay and Priestley's (1992) opinion, the influence of the shear effect on the plastic hinge length of RC columns is also significant. To consider the contribution of the shear effect to the plastic hinge length of RC columns, Paulay and Priestley (1992) took steel stress as a parameter together with the shear span ratio and reinforcement diameter. Bas (2005) conducted a series of tests on RC columns with large section sizes, which showed that it was a better way to describe the plastic hinge length of RC columns by the axial compression ratio, shear span ratio, and confining reinforcement ratio, which verified the opinions given by Wang *et al.* (1989). After analyzing the effect of concrete strength, reinforcement strength, and diameter on plastic hinge length individually, Berry *et al.* (2008) modified Park's formula to obtain more accurate results. Additionally, Bae and Bayrak (2008) thought the plastic hinge length was determined by the axial compression ratio, shear span ratio, and reinforcement ratio. Ou *et al.* (2012) believed that the plastic hinge length was related to the axial load, longitudinal reinforcement, and shear span ratio. However, according to the research results of Sun *et al.* (2011), the axial compression ratio, reinforcement strength, and reinforcement ratio had a slight effect on the plastic hinge length, which was governed by the column length, section width, and diameter of longitudinal steel. Moreover, Sakai and Hoshikuma (2014) tested 19 bridge columns and proposed a formula considering the reinforcement strength, stirrup constraint, and concrete cover thickness.

The previous studies on plastic hinge length mostly focused on the single state when a structure fails. Little attention has been paid to the propagation process of plastic hinges as loading proceeds and the influence of the size effect. In order to grasp the propagation of plastic hinges during earthquakes and explore the effect of section size on plastic hinges, six RC columns with different section sizes and axial compression ratios were tested quasi-statically. Based on the experimental results, the influence of the loading amplitude and size effect on the plastic hinge length of RC columns is discussed.

2. Test program

2.1 Details of specimens

The purpose of this test was to determine the influence of the axial compression ratio, loading increment, and size effect. In the specimen design, section size and axial compression ratio were considered carefully. Two axial compression ratios (n) of 0.4 and 0.6 were adopted. When $n=0.4$, three types of RC columns were constructed with the section sizes of 300 mm×300 mm, 500 mm×500 mm, and 700 mm×700 mm, which were labeled as Units 1-3. The shear span ratio was fixed at 0.4; thus, the heights of Units 1-3 were 1092 mm, 1820 mm, and 2548 mm, respectively. The longitudinal reinforcement and stirrup ratio of all specimens were held constant at 1.51% and 1.89%, respectively. To eliminate the effect of uncertainties, the other parameters of Units 1-3 were designed such that the same proportion of their section size (3:5:7) was maintained. When

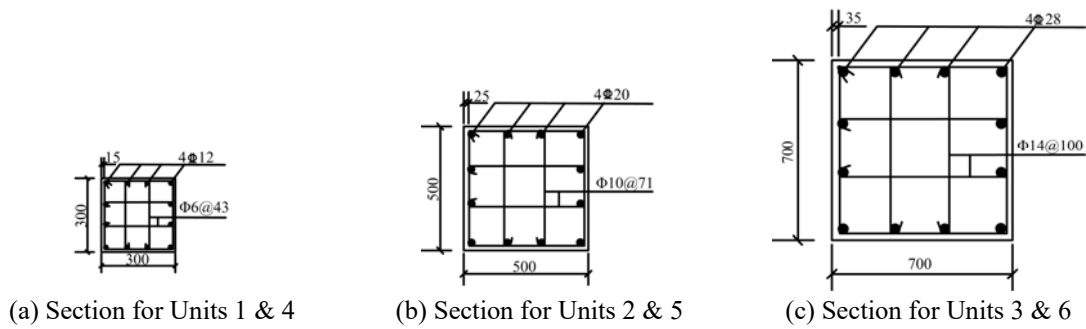


Fig. 1 Geometry and reinforcement details of test columns

Table 1 Parameters of specimens

Column Unit	Section Size (mm)	Height (mm)	Compressive Strength of Concrete (MPa)	Thickness of Concrete Cover (mm)	Longitudinal Reinforcement	Stirrup
1 & 4	300×300	1092	26	15	12Φ12	Φ6@43
2 & 5	500×500	1820	30	25	12Φ20	Φ10@71
3 & 6	700×700	2548	30	35	12Φ28	Φ14@100

Table 2 Mechanical properties of reinforcement rebars and concrete

Properties of Steel					
Specification	Yield Strength (MPa)	Ultimate Strength (MPa)	Yield Strain	Elastic Modulus (10 ⁵ MPa)	Elongation (%)
Φ12	433	606	2570	2.03	20.56
Φ20	424	589	2484	2.01	28.50
Φ28	422	616	2340	2.02	26.43
Concrete Compressive Strength (Mpa)					
Specimens with $n=0.4$			Specimens with $n=0.6$		
Unit 1	Unit 2	Unit 3	Unit 4	Unit 5	Unit 6
26	30	30	26	28	30

$n=0.6$, another three columns with the same parameters of Units 1-3 were constructed and labeled as Units 4-6. The dimensions and reinforcement details of all column units are shown in Fig. 1. For comparison, the main parameters of these specimens are listed in Table 1.

For all these specimens, C30 grade concrete (based on the Chinese design code (2010)) was chosen, which has a compressive strength of 30 N/mm^2 after 28 days. All reinforcement rebars used here were from Chinese Grade 345 steel (2010). The tested mechanical properties of the steel and concrete used in this test are listed in Table 2.

2.2 Loading and measurement system

2.2.1 Loading arrangements and testing procedure

All six column units were tested under constant axial load and cyclic bending. For Units 1 and 4, the concentric axial load was applied to the test column by a 2000 kN jack through a cylindrical steel bearing that allowed free rotation at the ends of column, as shown in Fig. 2(a), and the cyclic bending was simulated by a $\pm 1000 \text{ kN}$ jack mounted on the top ends of the columns horizontally. For Units 2, 3, 5, and 6, the axial loads approached 3000 kN-8820 kN, which exceeds the capacity of the conventional jack. These four columns were tested using the multi-functional electro-hydraulic testing machine at Beijing University of Technology. This machine equips a vertical jack on the top with a capacity of 100 MN and a reversible horizontal jack on the bottom with a capacity of $\pm 4000 \text{ kN}$. Thus, the loading system for Units 2, 3, 5, and 6 is as shown in Fig. 2(b). The axial load was applied to the test columns through a huge cylindrical steel bearing, and a horizontal force was loaded on the bottom of the test columns through a sliding block to simulate the cyclic bending.

2.2.2 Loading protocol

The concentric axial load was applied to the specimen at the beginning of the test and was kept at a constant value during the entire testing process. Afterward, lateral cyclic loads were applied quasi-statically through a horizontal actuator. The lateral loading protocol is shown in Fig. 3. Before the specimen yielded, the lateral loading was force controlled, and one cycle was

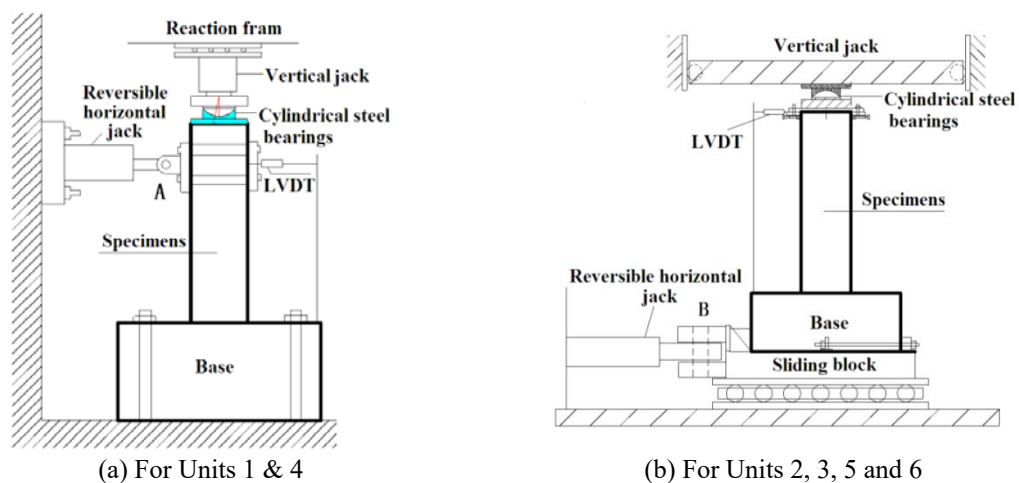


Fig. 2 Loading systems

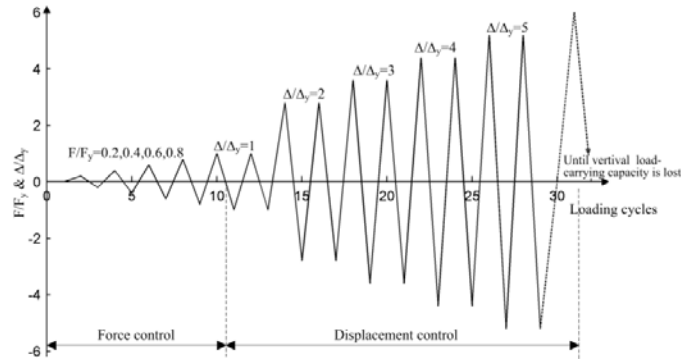


Fig. 3 Loading history



Fig. 4 Instrumentation positions

performed at each force level. In this phase, five levels with the loading interval of 0.2 times the predicted yield load F_y of the specimen were considered. After the specimen yielded, the loading was displacement controlled, and two cycles were repeated at each displacement level. The displacement loading amplitudes had an increment of $0.5\Delta_y$, where Δ_y denotes the predicted yield displacement of the specimen. In the test, push was defined as positive loading and pull as negative loading, and the order implemented was a push followed by a pull for each cycle. The loading was terminated when the specimen had no vertical load-carrying capacity as a result of the compressive crushing of concrete at the base of the column.

2.2.3 Instrumentation

In this test, measuring apparatuses were used to measure the loads, displacements, and strains of longitudinal steels. Load cells measured the vertical and lateral loads applied to the specimens. A linear variable differential transformer (LVDT) was set on the top of the tested column to obtain the lateral displacement, as shown in Fig. 2. To track the propagation of plastic hinge length, strain gauges and extensometers were used to monitor the strain response of longitudinal steels and the bending deformations in the plastic hinge zone. Fig. 4(a) shows the locations of the strain gauges on the columns. Four layers of strain gauges were attached in the region of $1.5h$ from the column base (h is the section height). The first layer (S1 and S2) was mounted at the location of 50mm up to the column base. The distance between the second layer (S3 and S4) and the first layer was $h/4$. The third (S5 and S6) and fourth layers (S7 and S8) were located at the points of three and six

times the hoop spacing (s) above the second layer, respectively. Fig. 4(b) shows the locations of the extensometers on the columns. Four extensometers were mounted 50 mm above the column base. The horizontal spacing (h_s) was the distance between the internal surfaces of the longitudinal rebars, and the vertical spacing (H_s) was about 0.5 times the section height.

3. Experimental results of plastic hinge length

3.1 Lateral force-displacement relationship

Fig. 5 shows the measured lateral force (P) versus displacement (Δ) relationships for all tested columns. The hysteresis loops of the RC columns were full, which demonstrated that all these columns were in flexural failure mode. In the following section, three states of each column were adopted to estimate the plastic hinge length, including yielding, peak load (P_m) and ultimate limit state (ULS) (defined as the state when the lateral load decreased to 85% of its peak value). All three states for each column are labeled in Fig. 5.

3.2 Measured plastic hinge length

Plastic hinge length is a nonobjective index that can only be measured indirectly based on other specific structural responses, such as displacement and strain. Normally, one of two methods is used to obtain the plastic hinge length (Li 2010). One is based on the strain response of the longitudinal rebars, measured by strain gauges; the other is based on the sectional curvature. In this section, both of them will be discussed.

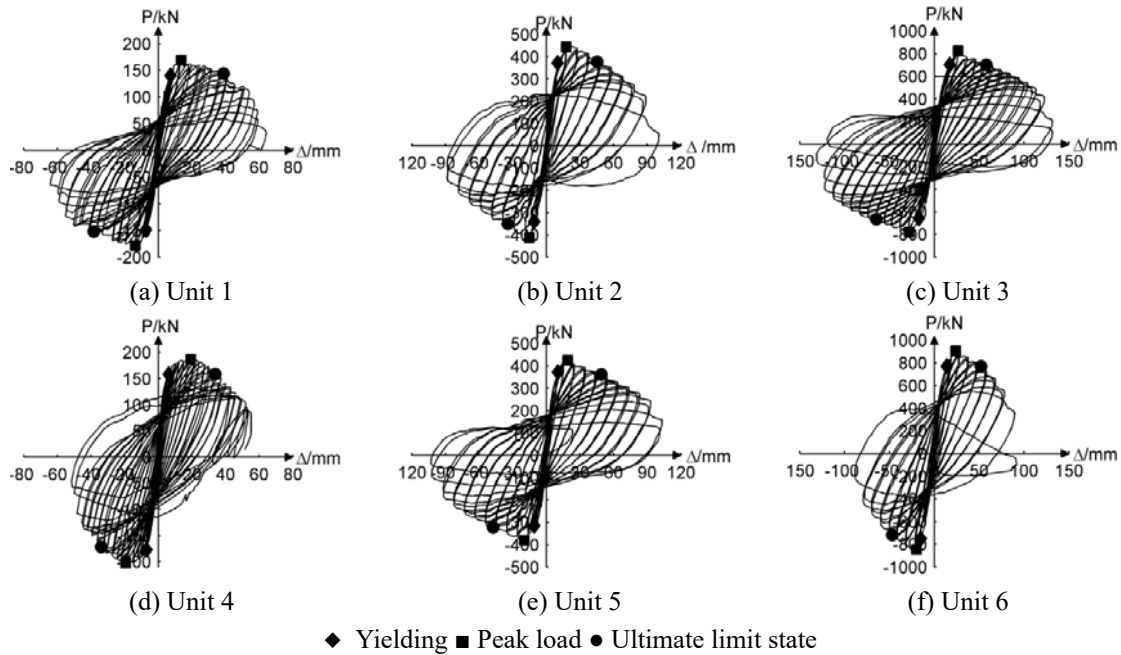


Fig. 5 Hysteresis loops for lateral force versus top displacement of specimens

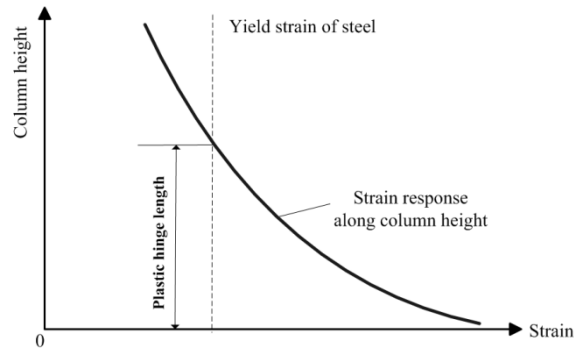


Fig. 6 Definition of plastic hinge length for RC column based on strain response of longitudinal rebars

3.2.1 Measuring based on strain of longitudinal rebars

First, the plastic hinge was used to describe the behavior of ideal elastic-plastic materials in which the inelastic deformation concentrates at a point. However, in RC components, the plastic hinge distributes over a particular zone. In an RC column, with the increase of deformation or load, the longitudinal rebars yield gradually along the column height. Then, the length of the yielded rebar is defined as the plastic hinge length of a column (Che *et al.* 2012) (see Fig. 6). For a given state, the strain responses of all sections of the longitudinal rebars represented by the solid line are obtained, and the height of the section whose strain response equals the yield strain of the used steel represented by the dashed line is determined to be the plastic hinge length of the column.

The plastic hinge of an RC column is below the region of $1.5h$ from the column base (Berry *et al.* 2008, Mendis 2001, Park *et al.* 1982). Hence, the tension strains monitored by the eight strain gauges shown in Fig. 4(a) were used to obtain the plastic hinge length. To track the propagation of the plastic hinge length for RC columns, seven states were extracted and plotted in Fig. 7 for both positive and negative loading. These included the three characteristic states labeled in Fig. 5, the two states of trisection displacement corresponding to yielding and peak load, and the two states of trisection displacement corresponding to peak load and ULS. These four states are represented by the solid line in Fig. 7. The tension strain was adopted. During cyclical loading, the rebar of one side was in tension when the horizontal jack pulled, while the rebar of the other side was in tension when the horizontal jack pushed. Hence, the left side of Fig. 7 plotted the tension strains measured by the strain gauges of S1, S3, S5, and S7 when the column was pulled, and the right side plotted the tension strains measured by the strain gauges of S2, S4, S6, and S8 when the column was pushed. The two strain gauges S1 and S2 close to the column base lost their functionalities before ULS, and thus, these two data related to ULS in Fig. 7 are missing. In the following section, the measured plastic hinge length corresponding to the 14 states presented in Fig. 7 will be used to investigate the propagation of plastic hinge length for RC columns. The other five columns showed the same results; therefore, Unit 3 was taken as an example here.

3.2.2 Measuring based on the sectional curvature

In the measurement of plastic hinge length based on the strain response of longitudinal rebars, the plastic hinge length is determined by the strain distribution of the rebars along the column height and the material yield strain of the steel used. Analogously, in the measurement based on the sectional curvature, the plastic hinge length depends on the curvature distribution along the

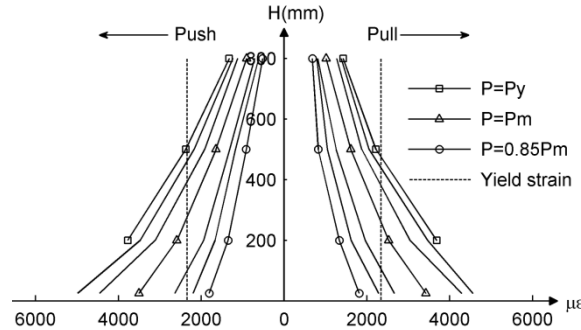


Fig. 7 Strain response of longitudinal rebars along column height for Unit 3

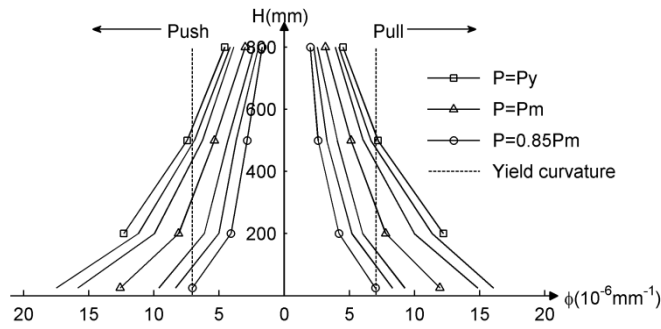


Fig. 8 Section curvature along column height for Unit 3 measured by strain gauges

column height and the yielded curvature of the bottom section of the column (Che *et al.* 2012). In this test, strain gauges and extensometers were used to monitor the sectional curvature.

Curvature measured by strain gauges: For a given section, the tension (ϵ_1) and compression strain (ϵ_2) can be measured by a pair of strain gauges. Then, the sectional curvature (ϕ) is governed by Eq. (1), where h_d is the longitudinal bar spacing, as shown in Fig. 4(a). The four pairs of strain gauges depicted in Fig. 4(a) measured the sectional curvature of the four sections. The same seven states in Fig. 7 were extracted and plotted in Fig. 8 for both positive and negative loading. For comparison, the tested results of Unit 3 are presented in Fig. 8

$$\phi = \frac{|\epsilon_1| + |\epsilon_2|}{h_d} \tag{1}$$

Curvature measured by extensometers: Unlike strain gauges, extensometers can measure the local response of a given section, and they are designed for measuring the relative displacement of a given zone. Hence, using the relative displacement (S_1 and S_2) measured by a pair of extensometers with h_s mounted in the range of H_s , the average curvature in this area can be obtained by Eq. (2). When H_s is quite small, the average curvature can represent the sectional curvature approximately. The two pairs of extensometers displayed in Fig. 4(b) measured the curvatures of two sections. The results of these states shown in Fig. 7 and Fig. 8 are summarized and presented in Fig. 9. The curvature of the bottom section cannot be obtained using this method;

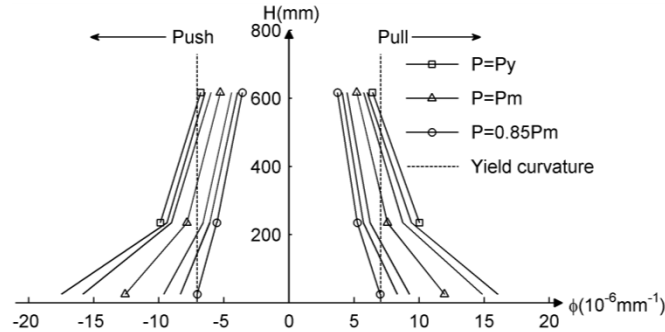


Fig. 9 Section curvature along column height for Unit 3 measured by extensometers

the presented points for this section in Fig. 9 were measured by strain gauges

$$\varphi = \frac{|S_1| + |S_2|}{H_s h_s} \tag{2}$$

The plastic hinge length of structural components is an important parameter for simulating the nonlinear structural response numerically using the finite element method. However, few experimental results have been reported so far. Thus, three methods were used to gain the plastic hinge length of an RC column to ensure the accuracy of the experimental results. The comparison of Figs. 7, 8, and 9 shows that these three methods gave the same plastic hinge lengths as the load increased, indicating that the measured plastic hinge length is accurate.

3.3 Equivalent plastic hinge length

Theoretical research (Priestley and Park 1987) is the main approach used in the investigation of plastic hinge length. To ascertain the difference between the authentic values and theoretical results, the typical computational method derived from the concept of equivalent plastic hinge length proposed by Priestley and Park (1987) was summarized for comparison. In this concept, the distribution pattern of the curvature for an RC column shown in Fig. 10(a) was assumed. This curvature distribution is considered to be composed of the yield curvature (φ_y) linearly distributed along the column height and the rectangular plastic curvature (φ_p) distributed in the plastic zone (l_{pe}), as shown in Fig. 10(b). That means the plastic curvature in the plastic zone is constant, and the plastic rotation equals $\varphi_p l_{pe}$. Meanwhile, the top displacement (Δ) of the column shown in Fig. 10(c) is composed of the yield displacement (Δ_y) and plastic displacement (Δ_p)

$$\Delta = \Delta_y + \Delta_p \tag{3}$$

where the yield displacement is

$$\Delta_y = \frac{1}{3} \varphi_y H^2 \tag{4}$$

and the plastic displacement is

$$\Delta_p = (\varphi - \varphi_y)l_{pe}(H - l_{pe} / 2) \tag{5}$$

Substitution of Eqs. (4) and (5) into Eq. (3) yields the top displacement of the column

$$\Delta = \varphi_y H^2 / 3 + (\varphi - \varphi_y)l_{pe}(H - l_{pe} / 2) \tag{6}$$

where H is the column height and φ is the curvature of the bottom section of the column. The equivalent plastic hinge length (l_{pe}) can be obtained from Eq. (6)

$$l_{pe} = H - \sqrt{H^2 - \frac{2(\Delta - \varphi_y H^2 / 3)}{\varphi - \varphi_y}} \tag{7}$$

The yield curvature is defined as

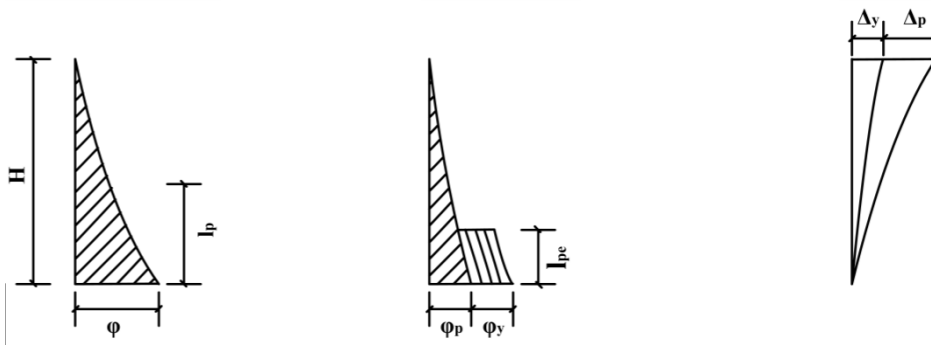
$$\varphi_y = \frac{\varepsilon_y}{(1 - \zeta_y) h_0} \tag{8}$$

in which ε_y is the yield strain of the longitudinal rebars and h_0 is the effective height of the section. The relative height of the compression zone ζ_y is governed by

$$\zeta_y = \frac{3\varepsilon_y n + \varepsilon_0}{3\varepsilon_y + \varepsilon_0} \tag{9}$$

where n represents the axial compression ratios. The strain (ε_0) corresponding to the peak strength of concrete is

$$\varepsilon_0 = \begin{cases} 0.002 + 0.5(f_{cu,k} - 50) \times 10^{-5} & (\varepsilon_0 \geq 0.002) \\ 0.002 & (\varepsilon_0 < 0.002) \end{cases} \tag{10}$$



(a) Assumed curvature distribution (b) Simplified curvature distribution (c) Top displacement of column

Fig. 10 Concept of equivalent plastic hinge length

where $f_{cu,k}$ is the characteristic value of the compressive strength of a 150 mm side length concrete cube. Thus, the plastic hinge length for any loading state can be estimated theoretically using Eq. (7). However, the curvature of the bottom section (φ) is not easily expressed for any state. Normally, the characteristic states, such as peak load and ULS, are given more attention. The equivalent plastic hinge lengths of these two states for the tested column were analyzed here. For the state at peak load, the curvature for the bottom section is set as

$$\varphi_{mp} = \frac{\varepsilon_{cu}}{x_m / 0.8} \tag{11}$$

where ε_{cu} is the ultimate compression strain of concrete (0.0033 here), and x_m is the depth of compression. For the state at ULS, the curvature for the bottom section is as

$$\varphi_{up} = \frac{\varepsilon_{cup}}{x_m / 0.8 - c} \tag{12}$$

and the parameter ε_{cup} is regarded as 1.5 times Mander’s research results (Mander *et al.* 1988)

$$\varepsilon_{cup} = 1.5 \left(0.004 + \left(1.4 \rho_s f_{yh} \varepsilon_{su} / f_{cc}' \right) \right) \tag{13}$$

where ρ_s and f_{yh} represent the volume–stirrup ratio and stirrup yield strength, respectively, ε_{su} is the ultimate strain of the stirrup (0.001 here), and c is the thickness of the concrete cover.

As discussed above, the equivalent plastic hinge length was determined by the geometrical and material parameters and the top displacement of the column. The measured lateral top displacement was adopted to estimate the plastic hinge lengths for the two states at peak load and ULS of all tested columns. The calculated values were depicted in Figs. 11 and 12 along with the results measured through strain gauges and extensometers, together with the concrete cracking and crushing of the column specimen after testing. Note that Methods 1, 2, and 3 represent the measurement of the plastic hinge length based on the strain of the longitudinal rebars, curvature

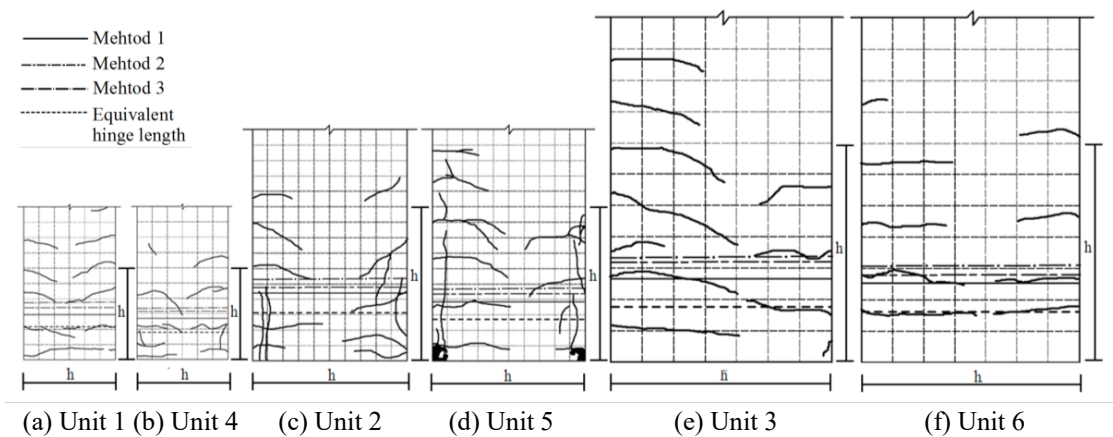


Fig. 11 Plastic hinge length for all tested column units at state of peak load

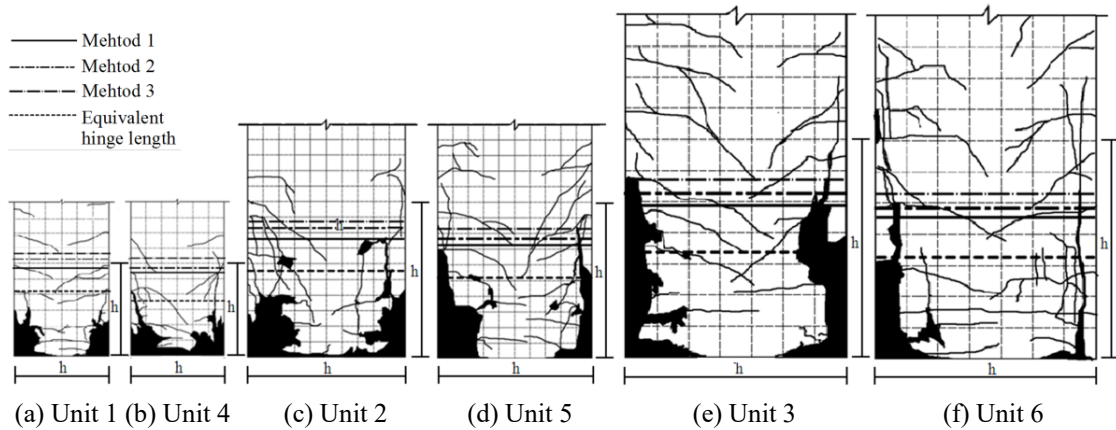


Fig. 12 Plastic hinge length for all tested column units at state of ULS

measured by strain gauges, and curvature measured by extensometers, respectively, hereinafter the same.

The comparison between Figs. 11 and 12 shows the plastic hinge length increases with loading but not by a constant value. Moreover, by contrasting the plastic hinge lengths of these columns with different section sizes, it can be found that the column with a larger section size had a smaller ratio of plastic hinge length relative to section height than the column with the smaller section size. This indicates that the size effect also plays an important role in the plastic hinge length of RC columns. The influence of loading and size effect will be examined in more detail in Sections 4 and 5, respectively.

4. Propagation of plastic hinge length

To sum up, the potential factors affecting the plastic hinge length include section size, material properties, reinforcement ratio, stirrup ratio, axial compression ratio, shear span ratio, and so on. In this work, an additional factor is considered: the propagation of the plastic hinge length as the loading proceeds. To explore the relation between plastic hinge lengths and loading amplitude individually, all the parameters except section size and axial compression ratio were designed to be the same for all tested column units. To eliminate the effect of section size, the relative plastic hinge length was used in this section, which was normalized by the column section height. The relative plastic hinge lengths of all states presented in Fig. 8 for each tested column unit were extracted, which were derived from the tested plastic hinge lengths based on the curvature measured by extensometers. The loading drift ratio was chosen to represent the loading amplitude. Fig. 13 shows the relative plastic hinge lengths (l_p/h) versus the loading drift ratios (θ). Meanwhile, the characteristic points related to the states of peak load and ULS for the pull and push sides were averaged and listed in Table 3 together with their relative equivalent plastic hinge lengths (l_{pe}/h).

In general, the plastic hinge lengths measured from the pull and push sides were highly consistent, as illustrated in Fig. 13. The plastic hinge lengths of all tested columns grew with increasing levels of loading drift, and they grew quickly at the beginning, but after approaching

peak load, the growth gradient was relatively small.

Many researchers (Gao and Pang 1987, Han *et al.* 2014, Wang *et al.* 1989) have concluded that higher axial compression ratios cause smaller plastic hinge lengths. This was also verified by the experimental results presented in Fig. 13 and Table 3. The plastic hinge lengths measured by Methods 1, 2, and 3 and the equivalent plastic hinge lengths all show that the column with $n=0.6$ got a larger value than that with $n=0.4$. However, Table 3 offers one more clue. The column with the higher axial compression ratio had a smaller plastic hinge length and a smaller loading drift ratio for the same states. For example, the drift ratios at ULS for Units 1, 2, and 3 with $n=0.4$ were 3.53, 2.647, and 2.41, respectively, while these values for Units 4, 5, and 6 with $n=0.6$ were 3.105, 2.185, and 1.938, respectively. That means the high axial compression ratio resulted in the low deformation capacity of the RC column, which has been verified by Watson and Park (1994) and Sheikh and Houry (1993). Herein, this factor was attributed to the effect of the loading amplitude characterized by the variable of the loading drift ratio.

All the experimental data points described in Fig. 13 were plotted in Fig. 14 as relative plastic hinge lengths (l_p/h) versus loading drift ratios (θ). It can be noted that the trend of l_p/h versus θ can be approximated by two straight lines with peak load (θ_m) as the division point. Based on the plotted points in Fig. 14, a bilinear model was obtained by curve fitting to describe the relation between the relative plastic hinge length and loading drift ratio

$$l_p/h = \begin{cases} 87.6\theta - 0.455 & (\theta \leq \theta_m) \\ 19.4\theta + 0.402 & (\theta > \theta_m) \end{cases} \tag{14}$$

Similarly, the characteristic points of the relative equivalent plastic hinge lengths listed in Table 3 were presented in Fig. 15, and a perfect linear equation was derived through curve fitting

$$l_{pe}/h = 16.4\theta + 0.12 \tag{15}$$

The data on relative equivalent plastic hinge lengths were started from the state of peak load; hence, there is only one linear plot in Fig. 15. Eqs. (14) and 15 clearly show that a bilinear model can describe the effect of loading on the plastic hinge length of an RC column accurately.

In addition, the approximate values of the plastic hinge length for the characteristic states at peak load and ULS are summarized in Table 3. Based on the measured data, the ranges of l_p at

Table 3 Relative plastic hinge length versus loading drift ratio

Column Unit	Drift ratio (10^{-2} rad)		l_p/h						l_{pe}/h		
	Peak load	ULS	Method 1		Method 2		Method 3		Peak load	ULS	
			Peak load	ULS	Peak load	ULS	Peak load	ULS			
$n=0.4$	1	1.247	3.533	0.497	0.963	0.57	1.037	0.633	1.117	0.363	0.707
	2	1.068	2.647	0.444	0.766	0.488	0.82	0.534	0.886	0.306	0.556
	3	1.067	2.410	0.384	0.703	0.431	0.76	0.484	0.814	0.257	0.487
$n=0.6$	4	1.078	3.105	0.45	0.907	0.517	0.96	0.56	1.047	0.303	0.61
	5	0.907	2.185	0.392	0.714	0.438	0.77	0.472	0.824	0.274	0.508
	6	0.858	1.938	0.364	0.644	0.401	0.697	0.433	0.759	0.236	0.461

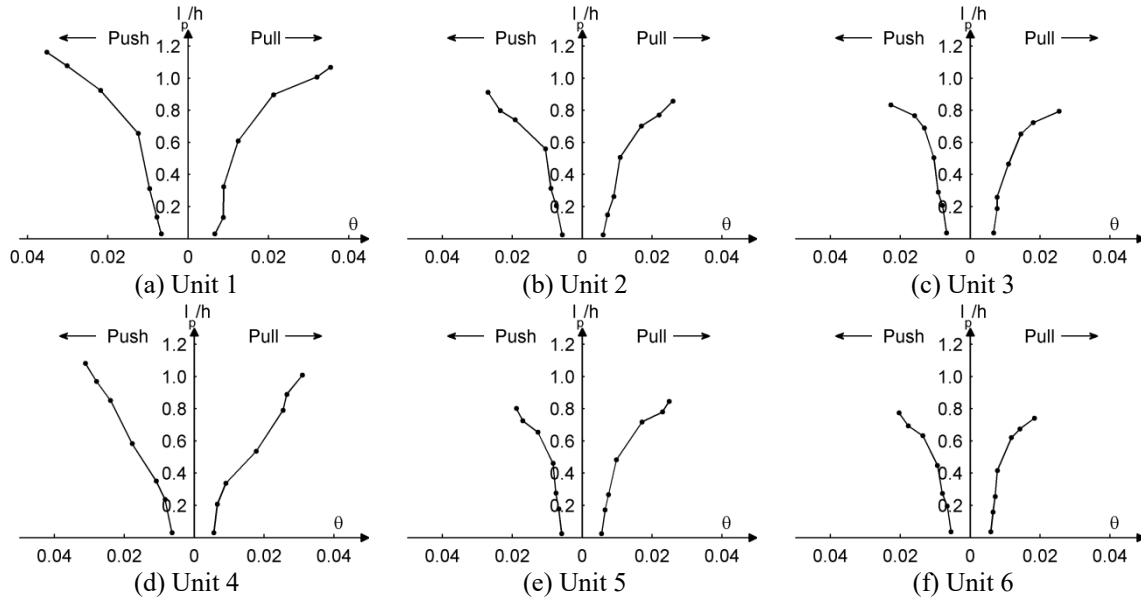


Fig. 13 Relative plastic hinge length versus loading drift ratio

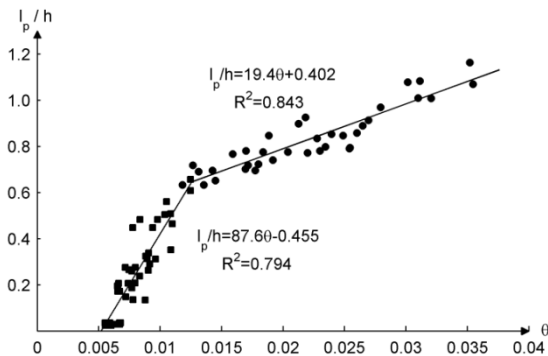


Fig. 14 Relationship between relative plastic hinge length and loading drift

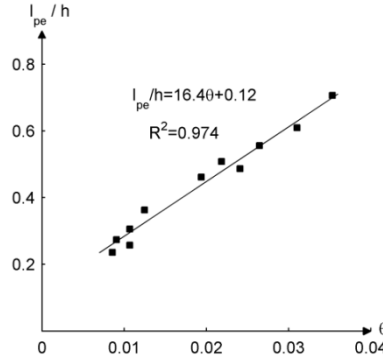


Fig. 15 Relationship between equivalent relative plastic hinge length and loading drift

peak load and ULS were $(0.364-0.633) h$ and $(0.644-1.117) h$, respectively, while the corresponding ranges of l_{pe} were $(0.236-0.363) h$ and $(0.461-0.707) h$.

5. Influence of size effect on plastic hinge length

The structural size effect is important to the correct interpretation of test data for larger real structures from a reduced scale. Many laboratory tests carried out on different scales have demonstrated that the size effect cannot be neglected when determining the mechanical properties of RC components (Agnieszka and Walraven 2002, Kim and Yi 2002). In this section, the influence of the size effect on the plastic hinge length of RC columns will be discussed briefly.

Fig. 16 shows the relationship between the relative equivalent plastic hinge length and the section height. It can be noted that the relative equivalent plastic hinge length, which has been normalized by section height, decreases distinctly as the section height increases. Compared to the column with $h=300$ mm when $n=0.4$, the l_p of the column with $h=500$ and 700 reduced by 13% and 26% in the state at peak load, respectively, and the reductions for the state at ULS were 19% and 28%, respectively. Meanwhile, when $n=0.6$, the trend was the same, demonstrating that the size effect needs to be considered when determining the plastic hinge length of RC columns

Banzant (1984) thought the size effect resulted from the energy release caused by fractures. The size effect was shown to consist of a smooth transition from the strength criterion for small sizes to linear elastic fracture mechanics for large sizes. In addition, a function was proposed to describe the decline of nominal stress. Based on his research, the plastic hinge length of RC columns considering the size effect (l_{pet}) can be calculated by

$$l_{pet} = \alpha_h l_{pe0}$$

$$\alpha_h = \frac{B_h}{\sqrt{1 + h/D_h}} \tag{16}$$

where l_{pe0} denotes the plastic hinge length of the standard specimen (the l_p of the column with $h=300$ was chosen in this work) and B_h and D_h are constant parameters related to the types of components. From the data points presented in Fig. 16, B_h and D_h were obtained by the least square method. When $B_h=1.72$ and $D_h=154$, the estimated curve has good agreement with the experimental data, as shown in Fig. 17. Hence, the size effect coefficient is governed by Eq. (17). After considering the size effect through Eqs. (16) and (17), the numerical plastic hinge length (l_{pec}) can be gained. The calculated values versus the experimental data displayed in Fig. 18 create an almost straight line at an angle of 45 degrees. This indicates that the calculated values matched the experimental data, and Eqs. (16) and (17) described the size effect existing in the plastic hinge length of RC columns successfully

$$\alpha_h = \begin{cases} 1 & (h \leq 300) \\ \frac{1.72}{\sqrt{1 + h/154}} & (h > 300) \end{cases} \tag{17}$$

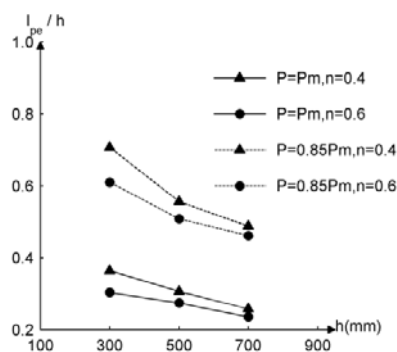


Fig. 16 Relative equivalent plastic hinge length versus section height

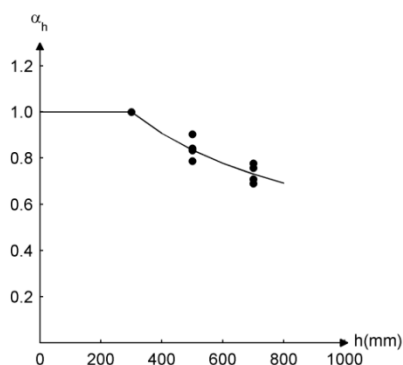


Fig. 17 Size effect coefficient for plastic hinge length

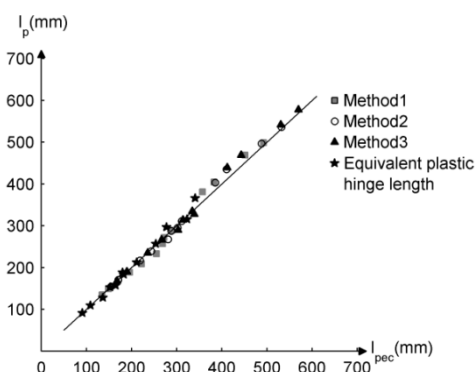


Fig. 18 Comparison of measured and calculated plastic hinge length considering size effect

6. Conclusions

This paper presented a series of quasi-static tests to examine the propagation of plastic hinge length for multi-scale RC columns considering the size effect. The following conclusions and recommendations are drawn from this study.

- The plastic hinge length was related to the loading procedures, which increased as the load proceeded after approaching the yield load. The growth gradient was larger before peak load than after. A bilinear model was obtained to describe the relationship between plastic hinge length and loading drift ratio.

- For the characteristic states at peak load and ULS, the ranges of plastic hinge length at peak load and ULS were $(0.364-0.633)h$ and $(0.644-1.117)h$, respectively, while the corresponding ranges of equivalent plastic hinge length were $(0.236-0.363)h$ and $(0.461-0.707)h$.

- The relative plastic hinge length decreased as the section height increased due to the size effect existing in RC components. When the section height varied from 300mm to 700mm, the plastic hinge length at the states of peak load and ULS reduced by 26% and 28%, respectively. Based on the theory of energy release, the size effect was considered successfully.

- The findings of this work can be embedded into the constitutive model for the distributed plastic hinge element and fiber element through the secondary development function of finite element analysis software. Then, the parametric effect of plastic hinge length on the global response of structure can be simulated in the structural nonlinear analysis.

Acknowledgments

The research described in this paper was financially supported by the National Natural Science Foundation of China (51178014) and the National Natural Science Foundation of China(51408378).

References

Agnieszka, B.V. and Walraven, J.C. (2002), "Size effects in plastic hinges of reinforced concrete members",

- Heron*, **47**(1), 53-75.
- Bae, S. (2005), "Seismic performance of full-scale reinforced concrete columns", Ph.D. Dissertation, University of Texas, Austin.
- Bae, S. and Bayrak, O. (2008), "Plastic hinge length of reinforced concrete columns", *ACI Struct. J.*, **105**(2), 123-133.
- Baker, A.L.L. (1956), *Ultimate Load Theory Applied to the Design of Reinforced and Prestressed Concrete Frames*, Concrete Publications, London, UK.
- Ban, S.Z. and Yamada, M. (1958), "Rotation limit of plastic hinge in reinforced concrete construction", *Trans. Architect. Inst. Japan*, **58**, 42-48.
- Bazant, Z.P. (1984), "Size effect in blunt fracture: concrete, rock, metal", *J. Eng. Mech.*, **110**(4), 518-535.
- Berry, M.P., Lehman, D.E. and Lowes, L.N. (2008), "Lumped-plasticity models for performance simulation of bridge columns", *ACI Struct. J.*, **105**(3), 270-279.
- Che, Y., Zheng, X.F., Wang, J.J. and Song, Y.P. (2012), "Size effect on flexural behavior of reinforced high-strength concrete beams subjected to monotonic loading", *J. Build. Struct.*, **33**(6), 96-102. (in Chinese)
- Chen, Z.H., Zhu, B.L. and Niu, H. (1984), "Nonlinear analysis of R.C. biaxial flexural-compression members", *China Civ. Eng. J.*, **17**(4), 67-78. (in Chinese)
- CMC. (2010), Code for Design of Concrete Structures (GB 50010-2010), China Ministry of Construction: Beijing, 19-20. (in Chinese)
- Gao, Z.S. and Pang, T.H. (1987), "Ductility and plastic hinge of the reinforced concrete frames", *J. Nanjing Inst. Technol.*, **17**(1), 106-117. (in Chinese)
- Han, Q., Zhou, Y.L., Du, X.L., Huang, C., George and Lee, C. (2014), "Experimental and numerical studies on seismic performance of hollow RC bridge columns", *Earthq. Struct.*, **3**(7), 251-269.
- Inel, M. and Ozmen, H.B. (2006), "Effects of plastic hinge properties in nonlinear analysis of reinforced concrete buildings", *Eng. Struct.*, **28**(11), 1494-1502.
- Kim, J.K. and Yi, S.T. (2002), "Application of size effect to compressive strength of concrete members", *Academy Proc. Eng. Sci.*, **27**(4), 467-484.
- Li, G.Q. (2010), "Experimental study and numerical analysis on seismic performance of reinforced concrete bridge columns", Ph.D. Dissertation, Chongqing Jiaotong University, China. (in Chinese)
- Mander, J.B., Priestley, M.J.N. and Park, R. (1988), "Theoretical stress-strain model for confined concrete", *J. Struct. Eng.*, **114**(8), 1804-1826.
- Mendis, P. (2001), "Plastic hinge lengths of normal and high-strength concrete in flexure", *Adv. Struct. Eng.*, **4**(4), 189-195.
- Mortezaei, A. (2013), "Plastic hinge length of RC columns considering soil-structure interaction", *Earthq. Struct.*, **6**(5), 679-702.
- Ou, Y.C., Kurniawan, R.A., Kurniawan, D.P. and Nguyen, N.D. (2012), "plastic hinge length of circular reinforced concrete columns", *Comput. Concrete*, **10**(6), 663-681.
- Park, R., Priestley, M.J.N. and Gill, W.D. (1982), "Ductility of square-confined concrete columns", *J. Struct. Div.*, **108**(ST4), 929-950.
- Paulay, T. and Priestley, M.J.N. (1992), *Seismic Design of Reinforced Concrete and Masonry Buildings*, Wiley-Interscience, New York, USA.
- Priestley, M.J.N. and Park, R. (1987), "Strength and ductility of concrete bridge columns under seismic loading", *ACI Struct. J.*, **84**(1), 61-76.
- Sakai, J. and Hoshikuma, S. (2014), "Evaluation of plastic hinge length of reinforced concrete bridge columns based on buckling behavior of longitudinal reinforcement", *Symposium Constr. Eng.*, **60A**, 782-795.
- Scott, M.H. and Fennes, G.L. (2006), "Plastic hinge integration methods for force-based beam-column elements", *J. Struct. Eng.*, **132**(2), 244-252.
- Sheikh, S.A. and Houry, S.S. (1993), "Confined concrete columns with stubs", *ACI Struct. J.*, **90**(4), 414-431.
- Shen, J.M. and Weng, Y.J. (1980), "The deformation and ductility of the reinforced concrete members", *J.*

- Build. Struct.*, **1**(2), 47-58. (in Chinese)
- Sun, Z.G., Wang, D.S., Guo, X. and Li, X.L. (2011), "Research on equivalent plastic hinge length of reinforced concrete bridge column", *China J. Highway Trans.*, **24**(5), 56-64. (in Chinese)
- Wang, F.M., Zeng, J.M. and Duan, L. (1989), "An experimental study of plastic hinge for reinforced concrete members with flexure and axial force", *J. Taiyuan Univ. Technol.*, **20**(4), 21-30. (in Chinese)
- Watson, S. and Park, R. (1994), "Simulated seismic load tests on reinforced concrete columns", *J. Struct. Eng.*, **120**(6), 1825-1849.
- Yang, K., Shi, Q.X. and Zhao, J.H. (2013), "Plastic hinge length of high-strength concrete columns confined by high-strength stirrups", *Eng. Mech.*, **30**(2), 254-259. (in Chinese)
- Zahn, F.A. (1985), "Design of reinforced concrete bridge columns for strength and ductility", Ph.D. Dissertation, University of Canterbury, Christchurch.

NM